

HfO_x/Al₂O₃ Bilayer RRAM with Enhanced Endurance and Synaptic Behavior with Highly Stable Potentiation/Depression Operation

Eric Yeu-Jer Lee, Kai-Chi Chuang, and Huang-Chung Cheng

Department of Electronics Engineering and Institute of Electronics, National Chiao Tung University,
1001 University Road, Hsinchu 30010, Taiwan, R.O.C.

Phone: +886-3-571-2121 ext. 31490 E-mail: ericleemaker@gmail.com

Abstract

TiN/Ti/HfO_x/Al₂O₃/TiN bilayer RRAM has been fabricated and studied. With the oxygen ions diffusion barrier Al₂O₃, the endurance and high resistive state (HRS) distribution have significant improvement compared to TiN/Ti/HfO_x/TiN RRAM with single resistive switching layer. Moreover, the bilayer RRAM shows highly stable potentiation/depression (P/D) operation characteristic. It exhibits gradual conductance change along with good linearity under 200 programming P/D cycles. Each cycle contains a train of 64 identical potentiation pulses (0.66V/100ns) and 64 identical depression pulses (-0.7V/100ns). Spike-timing-dependent plasticity (STDP) test is also demonstrated to show the device characteristic of biological learning.

1. Introduction

RRAM has been widely studied to develop as electronic synaptic devices due to its properties could be used in plenty artificial intelligence applications such as image recognition and auditory processing [1]. In order to emulate the synaptic behaviors, RRAM devices should exhibit a continuously gradual change in multiple resistance or conductance states corresponding to the change in synaptic weight strength [2].

In this study, the advantage of inserting Al₂O₃ layer which functioned as a diffusion limit layer (DLL) was first investigated through examining cumulative probability of low resistive state (LRS)/ high resistive state (HRS) and endurance [3]. In addition, to verify the synaptic characteristic of the bilayer RRAM, a train of identical potentiation and depression pulses were carried out to show the gradual conductance change. The nonlinearity weights of P/D progress were also fitted. At last, to explore the potential of bilayer RRAM in neuromorphic application based on Hebbian learning rule, STDP test was also demonstrated [4].

2. Experimental details

Resistive random access memory devices of TiN top electrode (TE)/Ti/HfO_x/Al₂O₃/TiN bottom electrode (BE) stack (Device A) with area 10μm×10μm were fabricated. First, a 6-inch silicon wafer with 500nm thermal oxide deposited by LPCVD was used as the substrate. Next, a 100-nm-thick TiN layer was deposited by RF sputtering and patterned to act as the BE. The resistive switching layer (RSL) composed of 2-nm-thick Al₂O₃ and 5-nm-thick HfO_x were deposited sequentially by ALD. A Ti layer was then deposited on the RSL to serve as the oxygen reservoir [5]. At last, a 100-nm-thick TiN was deposited using RF sputtering to act

as the TE. Lithography and dry etching were further conducted to complete the fabrication. Another TiN (TE)/Ti/HfO_x/TiN (BE) RRAM device (Device B) contained only a single 5-nm-thick HfO_x RSL with same effective device area was fabricated for comparison.

It is noted that the electrical characterization values including current, resistance and conductance in the all following experiments are all measured or converted under the 0.1V read voltage or 0.1V read pulse.

3. Results and discussion

Fig. 1 shows the direct current-voltage (I-V) curves of both Device A and B under 100 sweeping cycles.

To clarify the function of Al₂O₃ layer, the following experiments were conducted. Fig. 2(a) shows the cumulative probabilities of LRS/HRS after 100 DC sweeping cycles corresponding to Fig. 1. In HRS, the variance (δ/σ) was highly improved from 32% (Device B) to 16.91% (Device A). Moreover, Fig. 2(b) shows that device A exhibited a much better endurance up to 2×10^7 cycles before LRS failure compared to the endurance of device B which could only operate around 10^5 cycles. Both results indicated that the conductive filament (CF) could rupture stably and repeatedly in device A. These improvements could be attributed to the Al₂O₃ layer which limited the oxygen ions movement for not drifting randomly at the interface of HfO_x/Al₂O₃ to further cause uniform annihilation of oxygen vacancies during reset process. Therefore, Al₂O₃ could successfully serve as DLL in our experiments.

Fig. 3(a) shows one P/D cycle applied to device A which contained consecutive 64 identical potentiation pulses (0.66V/100ns) and 64 identical depression pulses (-0.7V/100ns). It reveals the conductance of device A could change gradually with a train of identical P/D pulses. Fig. 3(b) shows the nonlinearity weight fitting using *NeuroSim*+nonlinear weight update model [6]. The nonlinearity weight is 1.88 for potentiation and -2.12 for depression. This result indicates that the linearity is fairly good.

Fig. 4 shows stable gradual conductance change with good linearity and small cycle-to-cycle variation of device A while undergoing P/D cycles up to 200 (25600 pulses). Therefore, the desirable synaptic behavior of the bilayer RRAM was testified. This illustrated the adjustment of CF is very stable and consistent. Owing to the inserting Al₂O₃, device A could laterally modulate the width of CF by good control of oxygen ions movement to refill the oxygen vacancies properly at the HfO_x/Al₂O₃ interface [7]. The schematic diagram of the potentiation and depression processes was also

shown in Fig.4.

Fig. 5(a) shows the applied pre-spikes and post-spikes used for STDP measurement. The STDP behavior of device A was measured by carefully designed pre-spike pulses applied to the TiN TE, and post-spike pulses applied to the TiN BE. The conductance change (ΔW) of the device was then controlled by the net voltage drop which was the overlapped regions created by relative timing (Δt) of pre-spikes and post-spikes. Fig. 5(b) shows the measured conductance change (ΔW) as a function of Δt for device A. The measured data can be well fitted as follows:

$$\Delta W(\Delta t) = \begin{cases} a \times \exp(-\Delta t/\tau^+) & \text{if } \Delta t > 0 \\ b \times \exp(-\Delta t/\tau^-) & \text{if } \Delta t < 0 \end{cases}$$

a, b, τ^+ and τ^- are fitting parameters. The measurement result shows device A possessed the STDP characteristic to have the potential in biological learning application.

4. Conclusion

In summary, the TiN/Ti/HfO_x/Al₂O₃/TiN bilayer RRAM could have smaller fluctuation in HRS under DC sweep and the enhanced endurance due to the inserting Al₂O₃ functioning as the diffusion limiting layer of oxygen ions. Moreover, the consistent and stable lateral modulation of CF in potentiation and depression process could be fulfilled attributed to Al₂O₃ DLL. This makes HfO_x/Al₂O₃ bilayer RRAM exhibiting the gradual conductance change with fairly good linearity and small cycle-to-cycle variation while implementing the programming potentiation/depression cycles up to 200 (25600 pulses). At last, the STDP characteristic of the bilayer RRAM was also verified. These synaptic behaviors of HfO_x/Al₂O₃ RRAM suggest that the device is suitable for further neuromorphic applications.

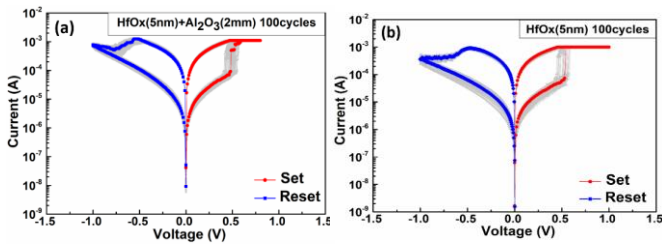


Fig. 1 Typical I-V curves of (a) HfO_x/Al₂O₃ bilayer RRAM and (b) HfO_x RRAM under 100 sweeping cycles.

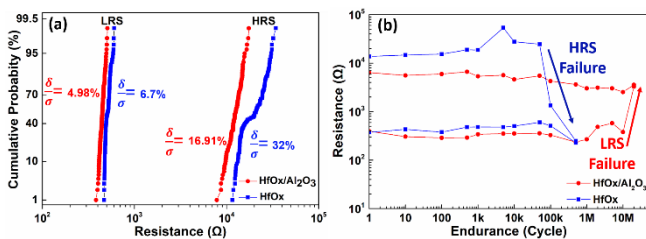


Fig. 2 (a) The cumulative probability of LRS/HRS under 100 DC cycles corresponding to Fig. 1 for device A and device B. The variance values (δ/σ) were shown in the figure. (b) The endurance of both devices. Operating parameters of device A: set pulse= 0.85V/100ns; reset pulse= -1.15V/500ns and device B: set pulse= 0.85V/100ns; reset pulse= -1.1V/500ns.

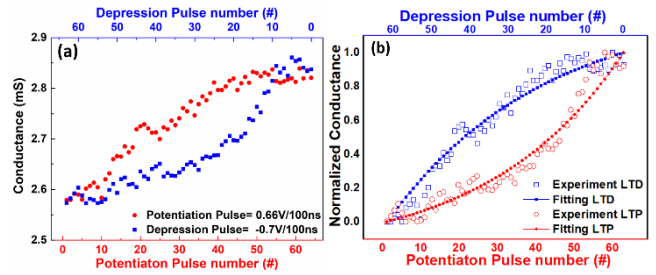


Fig. 3 (a) One Potentiation/Depression cycle contains a train of 64 identical positive voltage pulses (0.66V/100ns) followed by 64 identical negative voltage pulses (-0.7V/100ns). (b) The nonlinearity weight of long-term potentiation (LTP) is 1.88 and the nonlinearity weight of long-term depression (LTD) is -2.12.

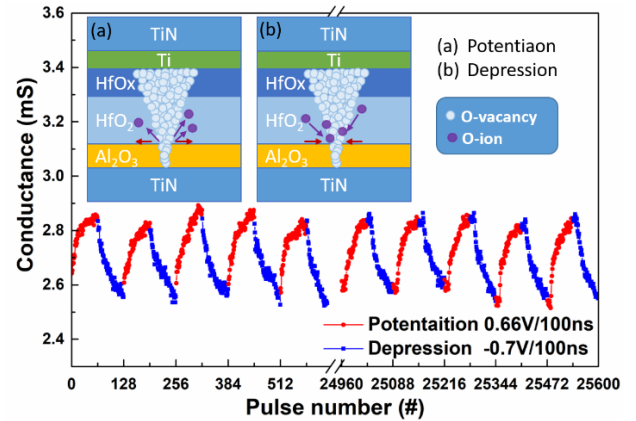


Fig. 4 The gradual conductance change of HfO_x/Al₂O₃ RRAM with good linearity and small cycle-to-cycle variation under 200 P/D programming cycles (25600 pulses). The lateral modulation of CF in potentiation and depression was demonstrated.

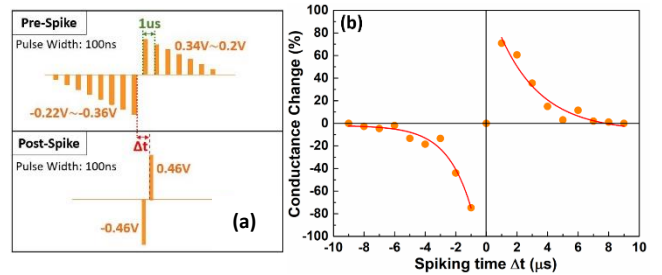


Fig. 5 (a) The applied pre-spikes and post-spikes used for STDP measurement. (b) The STDP measurement result shows the conductance change (synapse weight change) as a function of Δt .

References

- [1] S. Park *et al.*, IEDM Tech. Dig., (2012) pp. 231–234
- [2] J. Woo *et al.*, IEEE Electron Device Lett., vol. 38, no. 9 (2017) pp. 1220–1223
- [3] Z. Wang *et al.*, Nanoscale, vol. 8, no. 29 (2016) pp. 14015–14022
- [4] D.O. Hebb, *The Organization of Behavior: A Neuropsychological Study* (1949)
- [5] Zheng Fang *et al.*, IEEE Electron Device Lett., vol. 35, no. 9 (2014) pp. 914
- [6] P.-Y. Chen, X. Peng, S. Yu, *NeuroSim+: An integrated device-to-algorithm framework for benchmarking synaptic devices and array architectures*, IEDM, (2017)
- [7] Jiyong Woo *et al.*, IEEE Electron Device Lett., vol. 37, no. 8 (2016) pp. 995-996